ETH zürich

ETH Library

Factor XIII Cross-Linked Hyaluronan Hydrogels for Cartilage Tissue Engineering

Journal Article

Author(s):
Broguiere, Nicolas; Cavalli, Emma; Salzmann, Gian M.; Applegate, Lee A.; Zenobi-Wong, Marcy

Publication date:
2016-12-12

Permanent link:
https://doi.org/10.3929/ethz-b-000124354

Rights / license:
In Copyright - Non-Commercial Use Permitted

Originally published in:
ACS Biomaterials Science & Engineering 2(12), https://doi.org/10.1021/acsbiomaterials.6b00378

This page was generated automatically upon download from the ETH Zurich Research Collection.
For more information, please consult the Terms of use.

Factor XIII Cross-linked Hyaluronan Hydrogels for Cartilage Tissue Engineering

Nicolas Broguiere[†1], *Emma Cavalli*[†1], *Gian M. Salzmann*[2], *Lee Ann Applegate*[3], *Marcy Zenobi-Wong**[1]

† Equal contributions

Corresponding Author

*Email: marcy.zenobi@hest.ethz.ch. Address: HPL J20, Otto-Stern-Weg 7, 8093 Zürich

[1]ETH Zürich, Cartilage Engineering and Regeneration Laboratory, Switzerland

[2]Schulthess Klinik, Lengghalde 2, 8008 Zürich, Switzerland

[3]Department of Musculoskeletal Medicine, Regenerative Therapy Unit, University Hospital of Lausanne, Switzerland

Keywords: cartilage hyaluronan chondroprogenitors transglutaminase bioadhesive

In this study transglutaminase-crosslinked hyaluronan hydrogels (HA-TG) are investigated for their potential treating cartilage lesions. We show the hydrogels fulfill key requirements: they are simultaneously injectable, fast-gelling, biocompatible with encapsulated cells, mitogenic, chondroinductive, form-stable and strongly adhesive to native cartilage. Human

chondroprogenitors encapsulated in HA-TG gels simultaneously show good growth and chondrogenesis. Strikingly, within soft gels (~1 kPa), chondroprogenitors proliferate and deposit extracellular matrix to the extent that the hydrogels reach a modulus (~0.3 MPa) approaching that of native cartilage (~1 MPa) within 3 weeks. The combination of such off-the-shelf human chondroprogenitor cell line with HA-TG hydrogels lay the foundation for a cell-based treatment for cartilage lesions which is based on a minimally invasive one-step procedure, with improved reproducibility due to the defined cells, and with improved integration with the surrounding tissue due to the new hydrogel chemistry.

1. Introduction

Cartilage tissue has limited self-repair ability after injury or disease, which has prompted intensive efforts to engineer cell-based methods to regenerate the tissue.[1] In particular, matrix assisted autologous chondrocyte implantation (MACI) has been shown to be effective in comparison to microfracture,[2] but significant limitations and costs associated with cell expansion and two surgeries have prompted the search towards alternatives.[3] Single step procedures have been applied as early as 1982, when Albrecht and colleagues used autologous particulate cartilage pieces to treat articular joint surface defects.[4] This technique matured into a clinical product in the early 2000's with the introduction of cartilage autograft implantation system (CAIS) showing satisfying 2-year safety data.[5] Varying follow-up papers have shown general feasibility of minced autologous and allogeneic living cartilage pieces, with Christensen reporting 2-year data among a small collective of patients that have been treated with particulate cartilage pieces fixed by fibrin glue.[6] Clinical and MRI data showed good patient satisfaction and morphologically robust cartilage tissue formation.

Other approaches to further advance the treatment of cartilage lesions include development of injectable materials which can undergo in situ polymerization. GelrinC, based on polyethylene glycol (PEG) diacrylate and fibrinogen,[7] as well as the chitosan-based BS-Cargel are acellular products designed to enhance outcome of microfracture by providing a 3D environment for the repair cells.[8] Other injectable systems such as those based on albumin, hyaluronan (HA) and PEG (Novocart Inject [9]) are designed to be combined with autologous expanded chondrocytes. In addition the use of juvenile cartilage cells, considered immune-privileged and with great regenerative potential, has recently entered phase II clinical trials with promising results (RevaFlex™). In each clinical setting, an injectable material which is adhesive, chondrogenic and mitogenic is desired.[10] We recently reported the synthesis of novel HA-based injectable hydrogels which use the specific transglutaminase (TG) activity of the activated blood coagulation factor XIII (FXIIIa) for crosslinking.[11] The improved biocompatibility, gelling kinetics and adhesion due to this new cross-linking scheme are particularly attractive for cell delivery in cartilage applications. Furthermore, HA is a prominent component of cartilage tissue and is involved in many biological interactions (such as aggrecan binding to form large aggregates important for load bearing[12]) and signaling (through receptors such as CD44). Our synthesis is additionally based on high molecular weight HA which has been documented as anti-angiogenic, anti-oxidant and anti-inflammatory.[13]

Other HA based hydrogels have been described, such as those cross-linked with tyramines/HRP/hydrogen peroxide[14], methacrylates[15], aldehydes, thiols, and Huisgen cycloaddition, and have been reviewed[16]. In particular, photo-crosslinked HA hydrogels were shown to support chondrocyte matrix deposition and chondrogenic differentiation of mesenchymal stem cells (MSCs) both in vitro and in vivo. In direct comparison to relatively inert

poly(ethylene glycol) (PEG) hydrogels, with matched stiffness and same cross-linking chemistry, HA supported enhanced expression of cartilage-specific markers. The gene expression and matrix deposition found in methacrylated HA was close to what we obtain with chondroprogenitors in stiff HA-TG gels, however the authors did not investigate softer hydrogels, which give better results in our case, or the stiffening of the gels overtime due to matrix deposition.[15] Also, all of those cross-linking schemes have at least one drawback compared to the one presented here, in terms of specificity/toxicity, of gelling kinetics, of stability of the precursors in particular when working with high molecular weight HA, of adhesion to cartilage, or of ease of handling and injectability. Other enzymatically cross-linked hydrogels have been described as well[17] some of them enabling fast gel formation, low toxicity and adhesion to cartilage, but the amount of matrix deposition and the resulting gel stiffening observed in our system are still outstanding. For example, some recent work was published showing chondrocyte encapsulation in injectable carboxymethylated pullulan-chondroitin sulfate hydrogels. Fast gelling and good cell viability were demonstrated, but collagen 2 upregulation compared to 2D cultures, cartilage, or any other reference was not shown, collagen 2 deposition was only pericellular, and no gel stiffening resulting from matrix deposition was reported.[18]

In this paper, the HA-TG hydrogel is combined with human chondroprogenitor cells (hCCs) which were isolated by outgrowth culture from a 14 week fetal ulnar epiphysis. These cells have previously been shown to exhibit great homogeneity in expansion with steady proliferative potential[19] and produce phenotypically stable cartilage resistant to vascularization and mineralization in an in vivo subcutaneous mouse model.[20] hCCs also have low immunogenicity which makes them appropriate as an allogeneic off-the-shelf cell source where many patients can be treated in single step procedures from the same cell line.

2. Results and discussion The HA starting material as well as FXIII and thrombin are all in widespread use in the clinics, making it unlikely that any of the gel derivatives could create an immune response.[21] The fast and mild gelation makes the material particularly adapted to injection in situ, which would be optimum for clinical translation. For example, the gelling time for 1% (w/v) gels with 10 U/ml FXIIIa is on the order of ~30 s (time during which the precursor solution can be pipetted up and down after adding the enzyme until it forms a gel strong enough to clog the pipette) and no side reactions occur which could lead to toxicity due to the specificity of the enzyme.

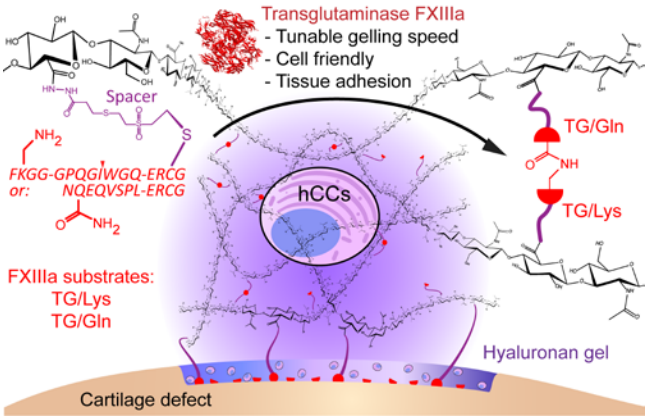

Figure 1. Concept schematics showing the gelation mechanism of transglutaminase (TG) cross-linked hyaluronan (HA). The lysine and glutamine residues that are covalently cross-linked by the TG FXIIIa are highlighted on the left, and the amide bond resulting from the conjugation is shown on the right. HA chains appear in black, peptides in red with reactive side chains explicitly shown, and the spacer/adapter between the peptides and the HA is in purple. Encapsulated human chondroprogenitor cells (hCCs) and adhesion to cartilage tissue are also represented.

The synthesis of the HA-TG precursors has been described in detail previously.[11] In short, HA was first thiolated using EDC activation and hydrazide conjugation of a dithiol containing

compound, followed by reduction of the dithiol with TCEP to yield HA-SH (Figure 2, Step 1). Then, a large excess of divinyl sulfone was added, to exchange the thiol functionality to vinyl sulfones (VS), yielding HA-VS. Finally, peptides containing a cysteine cassette were reacted onto the HA-VS, using again the efficiency of the Michael addition of thiols on VS (Figure 2, step 3). At every step, dialysis was the method of choice for removal of the buffers and unreacted small molecules, because it is very efficient with polymers and ensures no stress on the high MW HA chains, preserving the molecular weight.

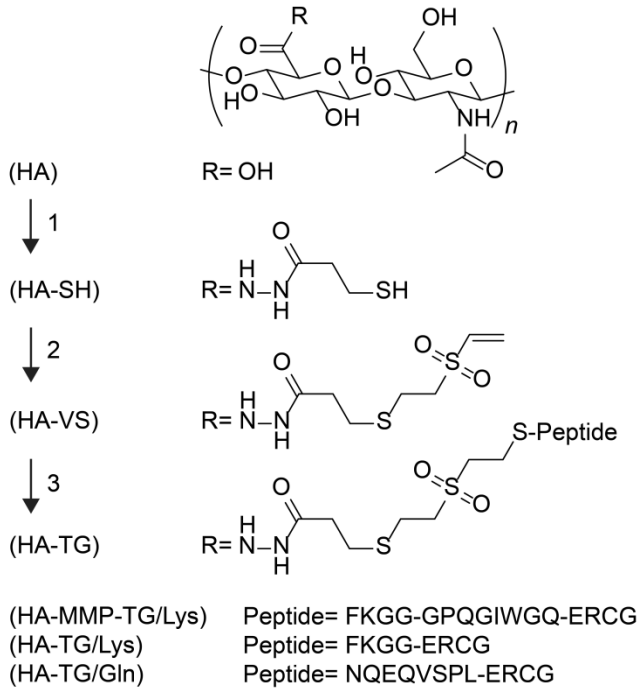

Figure 2. Chemical synthesis of HA-TG precursors. Reaction conditions are 1/ EDC, MES pH4.1 to 4.5, DTPHY then TCEP, 2/ DVS, TEOA pH8, 3/ Peptide, TEOA pH8.

To make gels with MMP sensitivity, we made a version of HA-TG that incorporated an MMP cleavable sequence within the TG/Lys peptide (Figure 2).

In this procedure, we targeted (through the amount of reagents in the first step) a substitution rate of 10%, which was confirmed by proton NMR on the HA-VS in D_2O as shown previously (VS peaks between 6 and 7 ppm versus acetylate peak from HA backbone at 1.9 ppm). Complete substitution of the HA-VS with peptides was confirmed by the complete disappearance of the VS peaks.

Since high molecular weight polymers and viscous solutions are difficult to analyze in details by NMR due to peak broadening, and since the HA-TG is an extreme case of such a solution, we treated the HA-TG precursor HA-TG/Lys with hyaluronidase at 10 U/ml overnight at 37ºC to partially hydrolyze the polysaccharide backbone and get clear NMR spectra. Reference spectra of unmodified HA, TG/Lys and DTPHY were used for peak identification, as well as previously published work on HA proton and carbon NMR.[22] To assign the peaks (especially on TG/Lys, for which no reference was known), the neighbors in the COSY spectrum together with multiplicity and integrals from the 1H spectrum were used. HSQC spectrum helped to distinguish overlapping peaks and was used to assign the carbons in the 13C spectrum. New peaks in the conjugate and cysteine beta-carbon shift show the creation of the linker and confirm the chemical structure (Supplementary Figures 7-10).

2.2. Mechanical characterization

The gelling behavior was characterized by rheometry (Figure 3A-B). Instead of pre-activating FXIII with thrombin as was done in the PEG literature, we reasoned that in situ activation of FXIII would give more interesting gelling kinetics. This way, a quite high amount of FXIII can be used, for very fast equilibration after activation, and the initial gelling speed can be tuned with the amount of thrombin, to have the gelling onset at the desired time (this can be seen as a cross-linking method having second order kinetics versus time instead of the usual linear progression).

It also means the same enzyme concentrations can be used for any macromer content, always yielding a similar gelation onset time. We chose to use 20 U/ml of FXIII and 12.5 U/ml of thrombin to obtain a gelation onset at around 1 min and an equilibration to a plateau after 10 min. In comparison, typical PEG gels formed by Michael addition typically have an onset of >10 min and equilibration in >1h at physiological pH.[23] The very high number of functional groups present on a single molecule, due to the high molecular weight of the HA precursor and 10% substitution rate, is expected to contribute largely to the fast gelation, together with the good kinetics of FXIIIa catalyzed cross-linking in general.

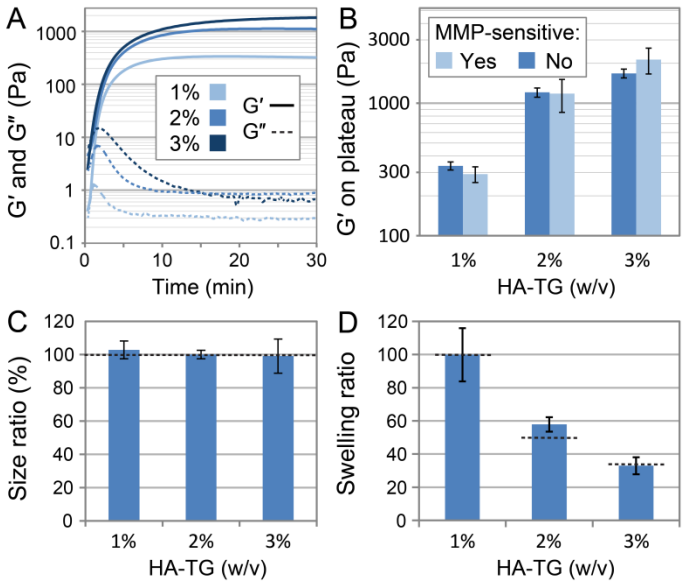

Figure 3. Material properties. (A) Representative gelling curves as monitored by rheometry showing the build-up of the storage G′ and loss G″ moduli for various concentrations of HA-TG. Note the fast gelation and equilibration to a plateau. (B) Values of the final storage modulus (taken at 30 min), showing the range of stiffness used in this study and the absence of influence from MMP sensitive sequence addition. (C) Change in diameter of the gels after 4 days of swelling in PBS. The dotted line indicates no change. (D) Swelling ratio (wet/dry weight of the

gels) after 4 days of swelling in PBS. The dotted line indicates the values expected for no mass loss or volume change. Error bars: SD with n=8 (for C and D at 3%) or n=3 (the rest).

Macromer precursor solutions of 1 to 3% gave storage moduli ranging from ~ 0.3 to 2 kPa, which span a range of stiffness that supported high cell viability. [23] Stable gels could still be formed down to at least 0.25% (w/v), but the high viscosity of the solutions at more than 3% makes the handling of more concentrated precursors difficult. There was no difference in mechanical properties of the HA-TG gel due to inclusion of the MMP-sensitive peptide.

Complete degradation of the gels could be achieved by treating them with either 10 U/ml hyaluronidase in PBS overnight at 37ºC, or 0.25% trypsin for 15 min at 37ºC. This indicates biodegradation is not hindered by TG cross-linking. The cells were nevertheless stable when used for cell cultures, as shown in the following sections.

Measurement of gel diameter and swelling ratios (dry mass over wet mass) showed that the gels did not undergo any dimensional change or polymer loss compared to D0 cast gels after incubation in PBS for 4 days (Figure 3C-D). The stable polymer content over 4 days demonstrates that essentially all HA chains were cross-linked, something which was expected for such a high number of functional groups per polymer chain. The lack of swelling or shrinkage, however, was a remarkable finding as it indicates a perfect balance of attraction and repulsion between the chains which allowed the gels to maintain their size at each concentration examined. Every part of the polymer chain likely plays a role in the auspicious shape stability, with negative charge on the HA contributing repulsion, peptides contributing positive charges, and the spacers hydrophobicity. As a partial confirmation of this reasoning, we measured the change in the diameter of HA-TG 1% gel disks when the ionic strength of the buffer is altered, which essentially changes the extent of shielding of the negative charge on the chains (Supplementary

Figure 4). As expected, gels immersed in ultrapure water increased in size while gels immersed in brine were shrinking (by approximately 200% and 10% respectively). The shape stability of HA-TG in physiological conditions is in contrast to most hydrogel systems where chain-chain and chain-solvent interactions lead to significant gel shrinkage or swelling. In these cases the unpredictable concentration- and time-dependent shape change can cause tissue engineered constructs to delaminate or pop out from their site of implantation.

2.3. Adhesion to cartilage explants

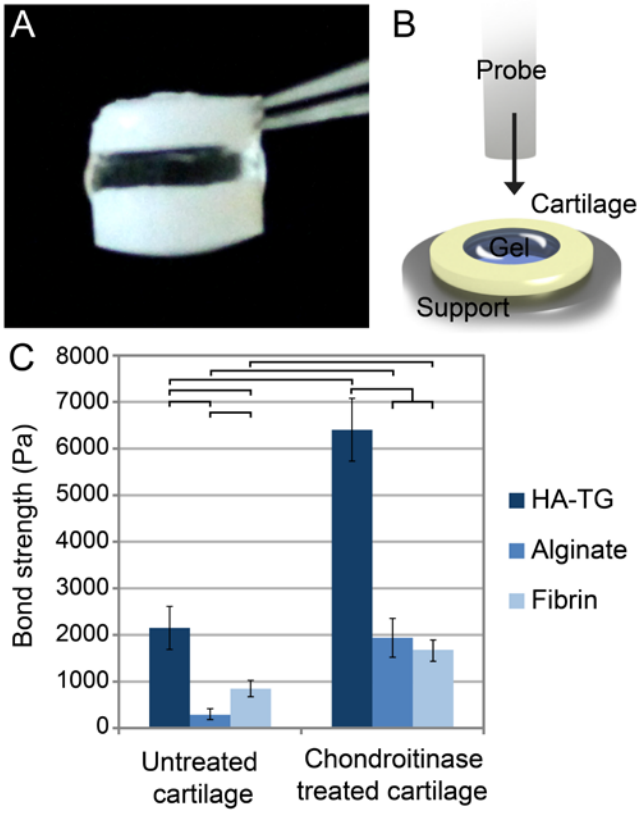

Figure 4. Adhesion to cartilage. (A) Cartilage biopsies adhered together with a gel layer. (B) Setup of the push-out assay for bond strength determination. (C) Bond strength of HA-TG gels compared with alginate and fibrin. Brackets: $p<0.05$. Error bars: SEM n=6.

Adhesion to cartilage explants was studied with push-out tests of cylinders of gels made in 4 mm rings of bovine cartilage (Figure 4). The adhesion was compared to fibrin, a common surgical glue and sealant,[24] and alginate, which is the most common hydrogel for 3D chondrocyte culture but is not adhesive.[25] The HA-TG was found to be significantly more adhesive to cartilage than fibrin glue, which was itself more adhesive than alginate (student t-tests $p<0.05$). When the cartilage surface was treated with chondroitinase, to remove the polysaccharides and expose the protein part of the cartilage matrix, which is what mediates the adhesion in all three cases, the adhesion strength was found to be increased by approximately 2, 3, and 6 fold for fibrin, HA-TG, and alginate respectively. Alginate and fibrin were becoming comparable, but HA-TG adhesion was ~3 times stronger than the controls, reaching a bond strength of more than 6 kPa.

2.4. Cartilage formation from encapsulated hCCs

Finally, hCCs were encapsulated in the hydrogels to study their potential to support chondrogenesis and effective cartilage tissue formation. These cells are particularly appealing for clinical translation due to their high chondrogenic potential and ability to treat many patients in a reproducible manner. They do not constitutively express cell surface molecules required for induction of T cell immune responses, and they were shown not to stimulate allogeneic T cells in vitro.[26] We analyzed the biological and mechanical outcome of hCCs in HA-TG cultures at 3 weeks post-encapsulation (D21). Alginate gels were used as controls.

Live/dead assays showed nearly full viability in all conditions (Figure 5A), and cell morphology as seen from calcein (whole cell) and actin staining (Figure 5B) was strongly dependent on polymer concentration. Cells spread and proliferated to fill almost the whole space in the softest gels, whereas they only formed small clusters without spreading in the stronger

gels. Confocal imaging of fluorescein tagged HA-TG gels (Supplementary Figure 5) showed that the pore size was under the resolution limit (~200 nm) in all conditions. The differences in cell spreading are therefore not directly explained by gel porosity, and have to involve gel deformation or degradation. Second harmonic generation (SHG) at 60 micron depth from the surface was collected simultaneously with calcein/PI fluorescence. This provided a way to check overall collagen production in a non-type-specific way directly amongst the living cells. The soft gels clearly stood out from the rest for being completely filled with a dense collagen network, whereas the other conditions just showed collagen deposition pericellularly. The collagen appeared fibrillar on the very surface of the gel, which is commonly seen from collagen 1 staining of such engineered cartilage constructs, but more homogeneous inside the gel, though it is deposited in the shape of the spread cells.

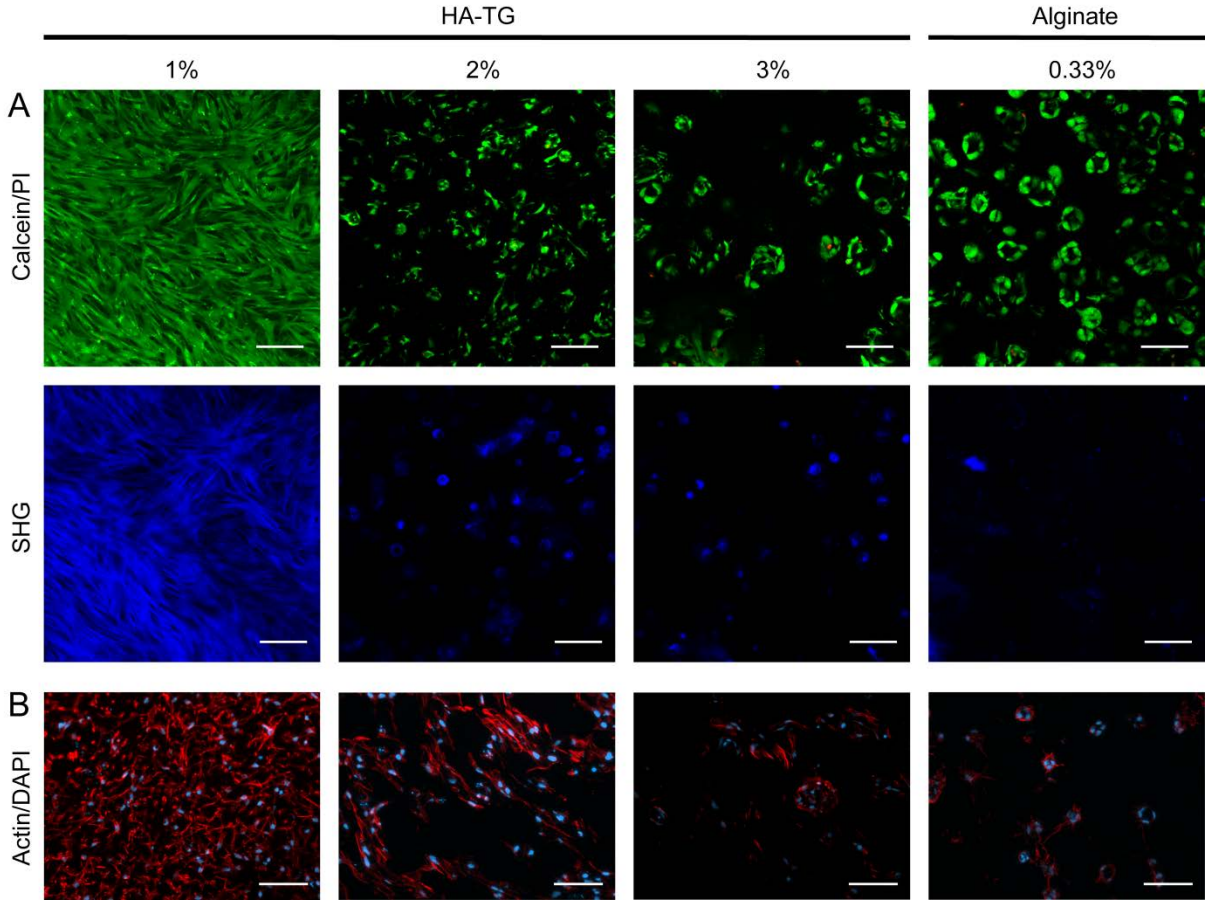

Figure 5. Cell and collagen morphology visualized with non-specific markers. (A) Multiphoton live imaging, with simultaneous acquisition of calcein (cytoplasm of live cells, green), propidium iodide (PI, nuclei of dead cells, red), and second harmonic generation (SHG, assembled collagen, blue). All conditions are highly viable, while cells spread, proliferate, and deposit a dense collagen matrix in soft HA-TG gels only. Images are aquired at ~60 μm depth beneath the surface of the gels. (B) Actin cytoskeleton (phalloidin, red) and nuclei (DAPI, blue) imaged in the center of the gels from fixed cryosections. This highlights that the spreading and proliferation of hCCs in soft HA-TG gels are not merely surface effects. (A+B) Images are at 21 days post encapsulation. Scale bars: 80 μm.

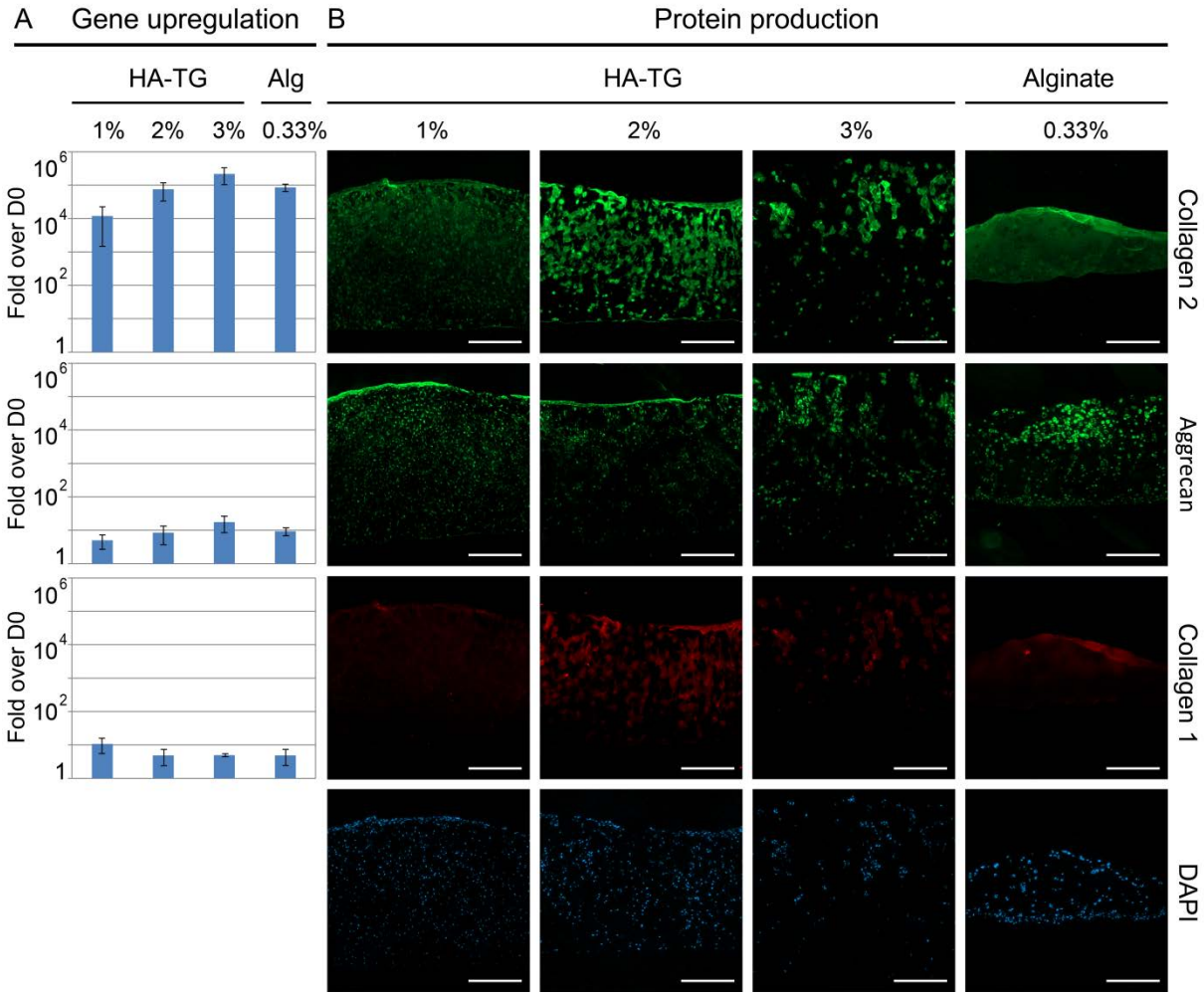

Figure 6. Cartilage production by encapsulated hCCs as seen from (A) gene expression 21 days post encapsulation, normalized to expression on the day of encapsulation (D0), and (B) matrix protein deposition. Each image is from a vertical slice of the gel taken from the center of the cylinder. Collagen 1, collagen 2 and DAPI are acquired on the same section. Scale bars: 400 μm.

We then investigated the matrix deposition at the gene and protein level with qPCR normalized to D0 and immunofluorescence, respectively (Figure 6). In all conditions, collagen 2 gene expression increased at least 10^4 fold, whereas collagen 1 upregulation was less than 10 fold, indicating good induction of chondrogenesis in all conditions. The high collagen 2 expression was also translated to the protein level: the soft gels were entirely filled with collagen 2 matrix, whereas the stiffer gels had only thin and more compact collagen 2 deposition around the cell clusters, reminiscent of what was seen in SHG. The collagen 2 / collagen 1 ratio was slightly higher in stiffer gels, which was expected as these cells had a rounder cell morphology.[27] Aggrecan was upregulated on the order of 10 fold in all conditions, again with higher expression in the stiffer gels. Aggrecan deposition was particularly strong on the HA gels surface. The most striking difference between the conditions is that the matrix deposition is more pericellular in stiffer gels and more homogeneous in softer gels.

The pattern of protein deposition was strongly depth-dependent, which can be attributed to that fact that the hydrogels were cultured in cylindrical PDMS casters bound to coverslips. The stainings clearly show proximity to the surface strongly benefits protein production, probably due to better access to nutrients/growth factors.

Finally, the most important outcome for clinical applications, the evolution of the mechanical properties over time, was evaluated (Figure 7). While it was found that stiff 3% gels essentially maintain their stiffness over the 3 week culture period, soft 1% gels showed a tremendous

increase in stiffness from an initial compressive modulus of ~1 kPa to a final value close to 0.3 MPa. Native cartilage measured in the same conditions was found to be ~1 MPa, consistent with reported literature values.[28] It is particularly noteworthy that the stiffness of the soft gels reached the order of magnitude of native cartilage in a clinically-relevant time frame. Intermediate 2% gels had values between these two extremes, and alginate gels were too unstable to be measured at D0 and only reached 10 kPa at D21. It is important to note that while the alginate gels underwent significant shrinkage and shape change, all of the HA-TG gels had nearly perfectly stable shape and size over the culture time. These stiffness results strongly correlate with the collagen deposition as seen by SHG that only shows assembled matrix, whereas gene expression was not the best predictor of physical outcome.

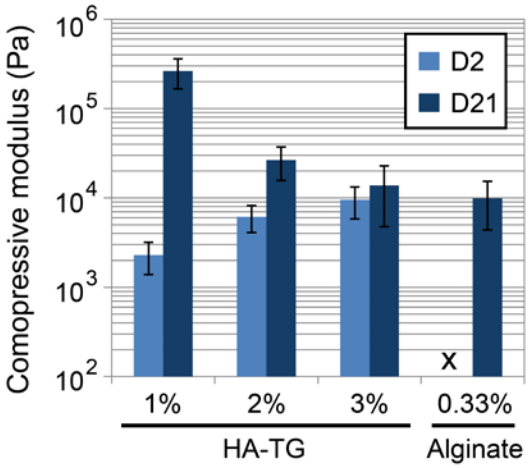

Figure 7. Evolution of the mechanical properties with matrix deposition by the hCCs between 2 and 21 days after encapsulation. Bovine hyaline cartilage was found to have a compressive modulus of 10^6 Pa in the same measuring conditions. Error bars: SD from n=3 (D2) and n=6 (D21).

All the cell experiments were performed as well with MMP sensitive HA-TG gels, and none of the characterizations showed a significant difference between MMP sensitive and insensitive

gels (data shown in Supplementary Figures 1-3). These results suggest that the increased cost and risk of premature gel degradation when using MMP sequences is not warranted, and that the use of HA-TG without MMP sequences is the best choice for cartilage tissue engineering.

3. Conclusion

We investigated the use of HA derivatives that can be cross-linked with the transglutaminase activity of FXIIIa for cartilage tissue engineering. We showed these gels have an ideal set of properties for treating cartilage lesions: they are injectable, very fast gelling, adhesive to cartilage tissue, retain their shape and have excellent biocompatibility. Human chondroprogenitors encapsulated in the gels showed tunable proliferation and good cartilage matrix deposition, transforming the gels into cartilage-like tissue within three weeks. Strikingly, the softest 1% gels showed a tremendous increase in stiffness over the culture time, reaching a stiffness of the same order of magnitude as native cartilage. The material development and in vitro characterization presented here support that HA-TG has potential for clinical translation, which would provide a 1-step treatment simpler than current standards, and should be brought forward to in vivo evaluation.

4. Experimental Section

All chemicals were purchased from Sigma-Aldrich and cell culture reagents from ThermoFisher Scientific unless stated otherwise.

HA-SH synthesis: 400 mg (1 mmol of the disaccharide repeat unit) of HA sodium salt (Lifecore Biomedical, 1.01-1.8 MDa), and 23.8 mg (0.1 mmol) of 3,3'-dithiobis(propanoic dihydrazide) (DTPHY, Frontier Scientific) were dissolved in a 150 mM MES solution with

occasional gentle swirling (final pH 4.1). Then 38.4 mg (0.2 mmol) of 1-ethyl-3-(3-dimethylaminopropyl)carbodiimide (EDC, Fluka) was dissolved in 1 ml of deionized water and added dropwise with stirring. The stirring was stopped and the reaction was allowed to continue overnight. The pH increased towards ~4.5 during the course of the reaction, with MES buffer preventing it from going higher. Then, 143.33 mg (0.5 mmol) of TCEP-HCl (Fluorochem) was dissolved in 500 μl water and added, the solution was homogenized by swirling, and the reduction was left to proceed overnight in a standing sealed flask. Finally, 1 g (17 mmol) of NaCl was added to the solution, and the mixture was dialyzed against ultrapure water balanced to pH 4.5 with dilute HCl, with 4 water changes over 24h, to yield a solution of pure HA-SH sodium salt.

HA-VS synthesis: The HA-SH solution recovered from the previous dialysis was added dropwise into a solution of 1 ml (10 mmol) divinyl sulfone (DVS) in 40 ml of triethanolamine (TEOA) buffer, 300 mM, pH 8.0. The reaction was left to proceed for 2h at RT, then 1 g of NaCl was added and the solution was dialyzed against ultrapure water to yield pure vinyl sulfone-substituted HA (HA-VS). The substitution rate was measured by comparing the peaks at 6.75 ppm (vinyl sulfones) and 1.75 ppm (N-acetyls from HA) from proton NMR in D_2O and found to be 10% of the carboxylic acids on HA.

HA-TG/Lys and HA-TG/Gln: The HA-VS was split in two equal parts. One half was substituted with a FXIIIa substrate peptide that provides a reactive glutamine residue (TG/Gln: NQEQVSPL-ERCG) and the other half with the peptide providing the reactive lysine (TG/Lys: FKGG -ERCG). For a matrix metallo-proteinase (MMP) sensitive version of the gels, a lysine donor with an MMP-sensitive sequence [29] was used instead (MMP-TG/Lys: FKGG-GPQGIWGQ-ERCG). Peptides (Anawa) contained ~40% salt which was taken into account in

the molarity calculations. For conjugation, 10 ml of TEOA buffer 300 mM, pH 8.0 was added to each HA-VS portion, the solutions were deoxygenated by bubbling with nitrogen gas, and finally the peptides were added at 1.3 excess over the VS. The solutions were quickly homogenized, the flasks sealed, and the reactions left to proceed overnight without stirring. Finally, 2 g of NaCl were dissolved in each flask, and the products were dialyzed against ultrapure water. The resulting pure HA-TG components were sterilized by 0.4 μm filtration, aliquoted, and lyophilized under sterile conditions. NMR spectra were acquired on a Bruker 600 Mhz instrument, using 15 to 25 mg of compound in 0.6 ml deuterated water, and spectra were analyzed using MestReNova.

HA-TG gel formation: Aliquots of HA-TG/Lys and HA-TG/Gln were resuspended at 1, 2, or 3% (w/v) in sterile filtered TBS (NaCl 150mM, CaCl2 50 mM, TRIS 50 mM, balanced to pH 7.6). Then, the two solutions were combined in equal volume to form HA-TG polymer stock. To trigger the gelation of 60 μl of HA-TG solution, 1.5 μl of thrombin solution (Baxter, 500 U/ml) followed by 6 μl of FXIII solution (Fibrogammin, CSL Behring, 200 U/ml) were added. Gelation occurred in ~1 min, which left enough time to transfer the liquid precursor.

Alginate gel formation: Alginate (Novamatrix) at 0.33% (w/v) (matching the stiffness of 3% HA-TG gels) in NaCl 150mM was placed in 4 mm diameter – 1 mm height cylindrical PDMS casters on coverslips, and gelled in ~500 μl of 100 mM CaCl2 solution for 1h, diffused through a pre-wetted membrane. The membrane and calcium were then removed and the gel covered with culture medium.

Shear moduli measurements: After adding the FXIII and thrombin, the gel precursor was quickly loaded onto an Anton Paar MCR 301 rheometer equipped with a 20 mm plate-plate geometry and metal floor, pre-warmed to 37°C and with humidified chamber. The probe was

quickly lowered to measuring position (0.1 to 0.2 mm, monitoring the gel precursor forming a ring around the geometry while lowering the probe to ensure the measuring space is precisely filled). The gelation was then monitored at 1 Hz with 4% strain, which was within the linear viscoelastic range of the gels (Supplementary Figure 6).

Compressive modulus measurements: Gels were left to swell for at least 2 days in PBS and tested under unconfined compression using a TA.XTplus Texture Analyzer (Stable Microsystems) with a 500 g load cell. The samples were compressed to a final strain of 10% at a rate of 0.01 mm/s. The compressive modulus E reported is the slope of the initial linear range of the stress-strain curve.

Adhesion strength measurements: Bovine articular cartilage samples with 1-2 mm thickness were harvested from the knee joints of calves aged 3-6 months. Cartilage rings of 8 mm in outer diameter and 4 mm inner diameter were prepared using biopsy punches and washed in PBS. The explants were then randomly divided in two groups: one group was left in PBS while the other was incubated for 15 minutes at 37°C in 1 U/ml chondroitinase ABC followed by 3 washes with PBS. The chondroitinase digestion results in approximately 50 µm digestion of GAGs as confirmed by Alcian blue staining (data not shown). Gels were injected into the circular hold of the cartilage explants and left to gel for 20 minutes at 37°C in a humidified chamber. To prevent leakage the explants were laid on a parafilm-coated surface. HA-TG gels were made as described at 3% (w/v), alginate gels at 1.5% (w/v) and gelled by immersion for 1h in a 100 mM calcium chloride solution, and fibrin gels contained 2% (w/v) fibrinogen and were gelled with 1 U/ml of thrombin for 1h at 37ºC. Push-out tests were performed at 0.5 mm/s rate with a 3 mm rod. The bond strength was calculated as the maximum force divided by the area of the inner punched hole.

hCCs isolation and expansion protocol: hCCs were harvested and isolated as described by Darwiche et al. Briefly, a tissue biopsy from the proximal ulnar epiphysis of a 14-week gestation donor was taken and minced. hCCs grew out of the tissue pieces. Cells were cultured for up to 2 weeks in DMEM (cat. 41966) containing 10% v/v FBS, 2mM L-glutamine, and 10 μg/ml Gentamycin. The cells were stored in liquid nitrogen, and expanded to passage 3 before encapsulation.

hCCs encapsulation in gels: Cells were trypsinized and resuspended at 15x106 cells/ml in the HA-TG solution, then the gelation was triggered as described previously. The gels were quickly cast in 4 mm diameter UV-sterilized PDMS cylindrical molds (SYLGARD 184, Corning) adhered to 10 mm coverslips. The gels were allowed to crosslink for 15 minutes at 37°C before adding chondrogenic medium (DMEM (cat. 31966) supplemented with 10 ng/ml transforming growth factor β3 (TGF-β3, Peprotech), 100 nM dexamethasone, 50 μg/ml L-ascorbate-2-phosphate, 40 μg/ml proline, 1% penicillin-streptomycin, and 1% ITS+ Premix (Corning)). The gels were incubated in a controlled humidified chamber (37°C, 5% (vol/vol) CO2) for 3 weeks and the culture media was replaced twice a week.

Live imaging: Gels were incubated for 1h in medium supplemented with 2 μM calcein AM and 6.6 μg/ml propidium iodide (PI), washed with fresh medium, and imaged on a Leica SP8 multiphoton microscope (25x water immersion objective, Mai Tai irradiation at 900 nm) with simultaneous collection of second harmonic generation (SHG) and fluorescence. The pictures presented were taken 60 to 70 μm from the sample surface, as the signal deteriorated at deeper depths.

Immunohistochemistry: Gels were fixed in 4% formaldehyde for 45 minutes, embedded in O.C.T (Tissue-Tek O.C.T Compound Blue, Sysmex) and stored at -80 °C. 5 μm thick sections

were cut using a Cryostat (CryoStar NX70, Thermo Scientific). Collagen 1 and 2 staining were performed after 30 minutes of 0.2% (w/v) hyaluronidase digestion at 37 °C and 1 hour blocking with 5% BSA in PBS with 1:200 diluted mouse anti-collagen 1 (Abcam #ab6308) and 1:200 diluted rabbit anti-collagen 2 (Rockland 600-401-104). Proteoglycan staining was performed after reducing the tissue with 10mM dithiothreitol in TBS pH 7.4 for 2 hours at 37ºC and alkylating with 40 mM iodoacetamide in PBS for 2 hours at 37°C. Sections were then digested with 0.02 U/ml chondroitinase ABC for 40 minutes at 37°C and blocked for 1 hour at room temperature with 5% BSA before incubating with primary antibody (Hybridoma 12/21/1-C-6). All primary antibodies were diluted in 1% (w/v) BSA in PBS and incubated overnight at 4°C. Alexa Fluor 594 Goat Anti-Mouse IgG (Invitrogen, A11005), Alexa Fluor 488 Goat anti-rabbit Alexa 488 (Invitrogen A11008) and Alexa Fluor 488 Goat anti-mouse (Invitrogen A11029) secondary antibodies were used at 1:200 dilution in 1% BSA in PBS for 1 hour at RT. Finally, slides were incubated for 10 minutes with the nuclear stain DAPI (Molecular Probes, Invitrogen) before mounting with VectaMount AQ Mounting Medium (Vector Laboratories).

RNA extraction and PCR: Samples were frozen in liquid nitrogen and crushed using pellet pestles (Thomas Scientific). Total RNA was prepared using NucleoSpin miRNA kit (Macherey-Nagel) and concentration was determined with a microplate reader Synergy H1 (BioTek Instruments). RNA with an absorbance ratio at 260/280 nm between 1.9 and 2.1 was used for PCR analysis. The Fast SYBR Green Master Mix (Applied Biosystems) was used to perform the PCR amplification with 150 nM forward and reverse primer. All primers (see Table 1) were designed across exon-exon junctions using Real Time PCR Design Tool from Integrated DNA Technologies (http://eu.idtdna.com/Scitools/Applications/RealTimePCR/Default.asp) to avoid the amplification of genomic DNA. All data came from 3 independent replicates and was

analyzed using the $2^{-\Delta\Delta Ct}$ method [30] and normalized against the reference gene RPL13a [31] with day 0 samples chosen as reference.

Table 1 Primer specification used for RT–PCR

mRNA	Accession n°	BP		Primer sequence (5'-3')
hRPL13a	NM_012423	100	FWD	AAGTACCAGGCAGTGACAG
			REV	CCTGTTTCCGTAGCCTCATG
hCol1a1	NM_000088	83	FWD	CAGCCGCTTCACCTACAGC
			REV	TTTTGTATTCAATCACTGTCGCC
hCol2a1	NM_001844	92	FWD	GGAATTCGGTGTGGACATAGG
			REV	ACTTGGGTCCTTTGGGTTTG
hCol10a1	NM_000493	108	FWD	ATTCCTAGTGGCTCCAATGTG
			REV	GCCTACCTCCATATGCATTTT
hACAN	NM_ 001135.3	98	FWD	GAATGGGAACCAGCCTATACC
			REV	TCTGTACTTTCCTCTGTTGCTG

Supporting Information

Supplementary figures showing hCCs in MMP sensitive HA-TG is available free of charge via the Internet at http://pubs.acs.org.

Acknowledgements

This work was supported by a CABMM startup grant, the ETH Zurich Foundation (Grant No. ETH-50 13-1), the Swiss National Science Foundation (Grant No. CR32I3_146338) and

FIFA/F-MARC (FIFA Medical Assessment and Research Center). We also acknowledge the help of the Scientific Center for Optical and Electron Microscopy (ScopeM) of ETH Zurich. The monoclonal antibody 12/21/1-C-6, developed by Caterson, B. was obtained from the Developmental Studies Hybridoma Bank, created by the NICHD of the NIH and maintained at The University of Iowa, Department of Biology, Iowa City, IA 52242.

References

1. (a) Becerra, J.; Andrades, J. A.; Guerado, E.; Zamora-Navas, P.; Lopez-Puertas, J. M.; Reddi, A. H., Articular cartilage: structure and regeneration. *Tissue Eng Part B Rev* **2010,** *16* (6), 617-27; (b) Makris, E. A.; Gomoll, A. H.; Malizos, K. N.; Hu, J. C.; Athanasiou, K. A., Repair and tissue engineering techniques for articular cartilage. *Nat Rev Rheumatol* **2015,** *11* (1), 21-34; (c) Ahmed, T. A.; Hincke, M. T., Strategies for articular cartilage lesion repair and functional restoration. *Tissue Eng Part B Rev* **2010,** *16* (3), 305-29.
2. (a) Basad, E.; Ishaque, B.; Bachmann, G.; Sturz, H.; Steinmeyer, J., Matrix-induced autologous chondrocyte implantation versus microfracture in the treatment of cartilage defects of the knee: a 2-year randomised study. *Knee Surg Sports Traumatol Arthrosc* **2010,** *18* (4), 519-27; (b) Saris, D.; Price, A.; Widuchowski, W.; Bertrand-Marchand, M.; Caron, J.; Drogset, J. O.; Emans, P.; Podskubka, A.; Tsuchida, A.; Kili, S.; Levine, D.; Brittberg, M.; group, S. s., Matrix-Applied Characterized Autologous Cultured Chondrocytes Versus Microfracture: Two-Year Follow-up of a Prospective Randomized Trial. *Am J Sports Med* **2014,** *42* (6), 1384-94.
3. Kon, E.; Filardo, G.; Di Martino, A.; Marcacci, M., ACI and MACI. *J Knee Surg* **2012,** *25* (1), 17-22.
4. (a) Albrecht, F. H., [Closure of joint cartilage defects using cartilage fragments and fibrin glue]. *Fortschr Med* **1983,** *101* (37), 1650-2; (b) Albrecht, F.; Roessner, A.; Zimmermann, E., Closure of osteochondral lesions using chondral fragments and fibrin adhesive. *Arch Orthop Trauma Surg* **1983,** *101* (3), 213-7.
5. (a) Cole, B. J.; Farr, J.; Winalski, C. S.; Hosea, T.; Richmond, J.; Mandelbaum, B.; De Deyne, P. G., Outcomes after a single-stage procedure for cell-based cartilage repair: a prospective clinical safety trial with 2-year follow-up. *Am J Sports Med* **2011,** *39* (6), 1170-9; (b) Farr, J.; Cole, B. J.; Sherman, S.; Karas, V., Particulated articular cartilage: CAIS and DeNovo NT. *J Knee Surg* **2012,** *25* (1), 23-9.
6. (a) Christensen, B. B.; Foldager, C. B.; Jensen, J.; Lind, M., Autologous Dual-Tissue Transplantation for Osteochondral Repair: Early Clinical and Radiological Results. *Cartilage* **2015,** *6* (3), 166-73; (b) Christensen, B. B.; Foldager, C. B.; Olesen, M. L.; Hede, K. C.; Lind, M., Implantation of Autologous Cartilage Chips Improves Cartilage Repair Tissue Quality in Osteochondral Defects: A Study in Gottingen Minipigs. *Am J Sports Med* **2016**.
7. Berdichevski, A.; Shachaf, Y.; Wechsler, R.; Seliktar, D., Protein composition alters in vivo resorption of PEG-based hydrogels as monitored by contrast-enhanced MRI. *Biomaterials* **2015,** *42*, 1-10.

8. (a) Stanish, W. D.; McCormack, R.; Forriol, F.; Mohtadi, N.; Pelet, S.; Desnoyers, J.; Restrepo, A.; Shive, M. S., Novel scaffold-based BST-CarGel treatment results in superior cartilage repair compared with microfracture in a randomized controlled trial. *J Bone Joint Surg Am* **2013,** *95* (18), 1640-50; (b) Shive, M. S.; Stanish, W. D.; McCormack, R.; Forriol, F.; Mohtadi, N.; Pelet, S.; Desnoyers, J.; Methot, S.; Vehik, K.; Restrepo, A., BST-CarGel(R) Treatment Maintains Cartilage Repair Superiority over Microfracture at 5 Years in a Multicenter Randomized Controlled Trial. *Cartilage* **2015,** *6* (2), 62-72.
9. Scholz, B.; Kinzelmann, C.; Benz, K.; Mollenhauer, J.; Wurst, H.; Schlosshauer, B., Suppression of adverse angiogenesis in an albumin-based hydrogel for articular cartilage and intervertebral disc regeneration. *Eur Cell Mater* **2010,** *20*, 24-36; discussion 36-7.
10. (a) Madeira, C.; Santhagunam, A.; Salgueiro, J. B.; Cabral, J. M., Advanced cell therapies for articular cartilage regeneration. *Trends Biotechnol* **2015,** *33* (1), 35-42; (b) Mardones, R.; Jofre, C. M.; Minguell, J. J., Cell Therapy and Tissue Engineering Approaches for Cartilage Repair and/or Regeneration. *Int J Stem Cells* **2015,** *8* (1), 48-53.
11. Broguiere, N.; Isenmann, L.; Zenobi-Wong, M., Novel enzymatically cross-linked hyaluronan hydrogels support the formation of 3D neuronal networks. *Biomaterials* **2016,** *99*, 47-55.
12. Allison, D. D.; Grande-Allen, K. J., Review. Hyaluronan: a powerful tissue engineering tool. *Tissue Eng* **2006,** *12* (8), 2131-40.
13. Masuko, K.; Murata, M.; Yudoh, K.; Kato, T.; Nakamura, H., Anti-inflammatory effects of hyaluronan in arthritis therapy: Not just for viscosity. *Int J Gen Med* **2009,** *2*, 77-81.
14. (a) Lee, F.; Chung, J. E.; Kurisawa, M., An injectable enzymatically crosslinked hyaluronic acid-tyramine hydrogel system with independent tuning of mechanical strength and gelation rate. *Soft Matter* **2008,** *4* (4), 880-887; (b) Jin, R.; Teixeira, L. S. M.; Dijkstra, P. J.; van Blitterswijk, C. A.; Karperien, M.; Feijen, J., Enzymatically-crosslinked injectable hydrogels based on biomimetic dextran-hyaluronic acid conjugates for cartilage tissue engineering. *Biomaterials* **2010,** *31* (11), 3103-3113; (c) Jin, R.; Teixeira, L. S. M.; Dijkstra, P. J.; van Blitterswijk, C. A.; Karperien, M.; Feijen, J., Chondrogenesis in injectable enzymatically crosslinked heparin/dextran hydrogels. *J Control Release* **2011,** *152* (1), 186-195.
15. Chung, C.; Burdick, J. A., Influence of Three-Dimensional Hyaluronic Acid Microenvironments on Mesenchymal Stem Cell Chondrogenesis. *Tissue Eng Pt A* **2009,** *15* (2), 243-254.
16. Burdick, J. A.; Prestwich, G. D., Hyaluronic Acid Hydrogels for Biomedical Applications. *Adv Mater* **2011,** *23* (12), H41-H56.
17. Teixeira, L. S.; Feijen, J.; van Blitterswijk, C. A.; Dijkstra, P. J.; Karperien, M., Enzyme-catalyzed crosslinkable hydrogels: emerging strategies for tissue engineering. *Biomaterials* **2012,** *33* (5), 1281-90.
18. Chen, F.; Yu, S. R.; Liu, B.; Ni, Y. Z.; Yu, C. Y.; Su, Y.; Zhu, X. Y.; Yu, X. W.; Zhou, Y. F.; Yan, D. Y., An Injectable Enzymatically Crosslinked Carboxymethylated Pullulan/Chondroitin Sulfate Hydrogel for Cartilage Tissue Engineering. *Sci Rep-Uk* **2016,** *6*.
19. Darwiche, S.; Scaletta, C.; Raffoul, W.; Pioletti, D. P.; Applegate, L. A., Epiphyseal Chondroprogenitors Provide a Stable Cell Source for Cartilage Cell Therapy. *Cell Med* **2012,** *4* (1), 23-32.
20. Studer, D.; Cavalli, E.; Formica, F. A.; Kuhn, G. A.; Salzmann, G.; Mumme, M.; Steinwachs, M. R.; Laurent-Applegate, L. A.; Maniura-Weber, K.; Zenobi-Wong, M., Human

chondroprogenitors in alginate-collagen hybrid scaffolds produce stable cartilage in vivo. *Journal of tissue engineering and regenerative medicine* **2016,** DOI: 10.1002/term.2203.
21. Reynolds, T. C.; Butine, M. D.; Visich, J. E.; Gunewardena, K. A.; MacMahon, M.; Pederson, S.; Bishop, P. D.; Morton, K. M., Safety, pharmacokinetics, and immunogenicity of single-dose rFXIII administration to healthy volunteers. *Journal of thrombosis and haemostasis : JTH* **2005,** *3* (5), 922-8.
22. (a) Pfeiler, E.; Toyoda, H.; Williams, M. D.; Nieman, R. A., Identification, structural analysis and function of hyaluronan in developing fish larvae (leptocephali). *Comparative biochemistry and physiology. Part B, Biochemistry & molecular biology* **2002,** *132* (2), 443-51; (b) Scott, J. E.; Heatley, F., Biological properties of hyaluronan in aqueous solution are controlled and sequestered by reversible tertiary structures, defined by NMR spectroscopy. *Biomacromolecules* **2002,** *3* (3), 547-53.
23. Lutolf, M. P.; Hubbell, J. A., Synthesis and physicochemical characterization of end-linked poly(ethylene glycol)-co-peptide hydrogels formed by Michael-type addition. *Biomacromolecules* **2003,** *4* (3), 713-22.
24. (a) Kim, M. K.; Choi, S. W.; Kim, S. R.; Oh, I. S.; Won, M. H., Autologous chondrocyte implantation in the knee using fibrin. *Knee Surg Sports Traumatol Arthrosc* **2010,** *18* (4), 528-34; (b) Patel, S.; Rodriguez-Merchan, E. C.; Haddad, F. S., The use of fibrin glue in surgery of the knee. *J Bone Joint Surg Br* **2010,** *92* (10), 1325-31.
25. (a) Kuo, C. K.; Ma, P. X., Ionically crosslinked alginate hydrogels as scaffolds for tissue engineering: part 1. Structure, gelation rate and mechanical properties. *Biomaterials* **2001,** *22* (6), 511-21; (b) Drury, J. L.; Mooney, D. J., Hydrogels for tissue engineering: scaffold design variables and applications. *Biomaterials* **2003,** *24* (24), 4337-51.
26. Adkisson, H. D.; Milliman, C.; Zhang, X.; Mauch, K.; Maziarz, R. T.; Streeter, P. R., Immune evasion by neocartilage-derived chondrocytes: Implications for biologic repair of joint articular cartilage. *Stem Cell Res* **2010,** *4* (1), 57-68.
27. Cao, B.; Peng, R.; Li, Z.; Ding, J., Effects of spreading areas and aspect ratios of single cells on dedifferentiation of chondrocytes. *Biomaterials* **2014,** *35* (25), 6871-81.
28. Park, S.; Hung, C. T.; Ateshian, G. A., Mechanical response of bovine articular cartilage under dynamic unconfined compression loading at physiological stress levels. *Osteoarthritis Cartilage* **2004,** *12* (1), 65-73.
29. Lutolf, M. P.; Hubbell, J. A., Synthetic biomaterials as instructive extracellular microenvironments for morphogenesis in tissue engineering. *Nat Biotechnol* **2005,** *23* (1), 47-55.
30. Matsiko, A.; Levingstone, T. J.; O'Brien, F. J.; Gleeson, J. P., Addition of hyaluronic acid improves cellular infiltration and promotes early-stage chondrogenesis in a collagen-based scaffold for cartilage tissue engineering. *J Mech Behav Biomed Mater* **2012,** *11*, 41-52.
31. Studer, D.; Lischer, S.; Jochum, W.; Ehrbar, M.; Zenobi-Wong, M.; Maniura-Weber, K., Ribosomal protein l13a as a reference gene for human bone marrow-derived mesenchymal stromal cells during expansion, adipo-, chondro-, and osteogenesis. *Tissue Eng Part C Methods* **2012,** *18* (10), 761-71.

New hyaluronan-based hydrogels cross-linked with the transglutaminase factor XIII, together with human chondroprogenitor cells, are used for cartilage tissue engineering. The gels are
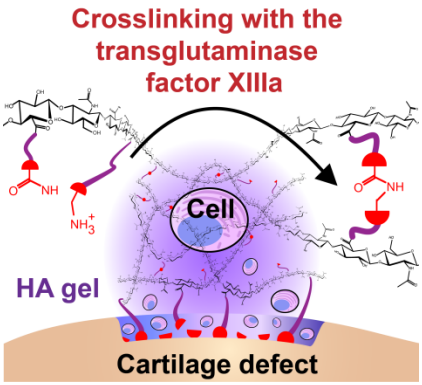
injectable, adhere to cartilage, keep encapsulated cells highly viable, retain their shape and promote cell proliferation and chondrogenesis. Initially soft gels with cells reach a stiffness of the same order of magnitude as native cartilage after 3 weeks of culture.